MAGNETIC FIELDS BEHIND CHONDRULE-FORMING PLANETARY BOW SHOCKS Chuhong Mai[1], Steve Desch[1] and Aaron Boley[2] [1]School of Earth and Space Exploration, Arizona State University, PO Box 871404, Tempe AZ 85287-1404 [2]Department of Physics and Astronomy, University of British Columbia, 6224 Agricultural Road, Vancouver BC V6T 1Z1 (chuhong.mai@asu.edu)

Introduction: Recent advances have allowed the measurement of the extremely weak remanent magnetizations present in chondrules, the millimeter-sized igneous spherules found in profusion in chondrites [1]. About 10% of chondrules in the Semarkona L3.0 chondrite have olivine phenocrysts ("dusty olivines") that contain iron-nickel metal (kamacite and tetrataenite) inclusions that retain magnetizations. These metal inclusions had to form as the (mostly silicate) chondrules themselves cooled below their liquidus temperatures (≈1700 °C) and started to crystallize. Because the directions of the magnetizations are consistent within a chondrule but vary from one chondrule to the next, the magnetizations must have been acquired while chondrules were freely floating objects in the solar nebula, before they were assembled into the chondrite parent body. Each chondrule's magnetization had to be acquired as it cooled below the Curie point of kamacite, ≈765 °C. An analysis of the remanent magnetization of chondrules in Semarkona shows they were magnetized by a nebular field $B \approx 54 \pm 21\ \mu T = 0.54 \pm 0.21$ G [1]. In contrast, chondrules in the CR chondrite LAP02342 cooled in a background field < 15 μT [2].

These remarkable measurements could be used to probe the background magnetic field of the solar nebula at the time and locations where ordinary and CR chondrites formed, *if* it were known how the magnetic field in the chondrule formation region differed from the ambient magnetic field. This requires modeling the chondrule-forming event, and the evolution of the magnetic field during chondrule formation. For that matter, measurements of the magnetic fields experienced by chondrules during their formation can rule out certain chondrule formation mechanisms.

Although it is not the only possible formation mechanism, and more than one mechanism may have operated, the majority of chondrules appear to have been melted by passage through shock waves in the solar nebula [3]. Shock waves tend to amplify the magnetic field as they compress the gas. They could be very large in extent and essentially one-dimensional, perhaps driven by gravitational instabilities; such shocks have been modeled by [4,5], among others. The behavior of the magnetic field in 1D shocks is simple: behind the shock, the magnetic field strength is proportional to the gas density (assuming the shock propagates perpendicular to the B field), regardless of the details of magnetic diffusion.

It is also possible that chondrules were melted by bow shocks caused by large planetary embryos on eccentric orbits [6,7]. These shocks are decidedly not one-dimensional, and magnetic diffusion (in the lateral direction) is important in this geometry. Chondrules will record the magnetic field at a point far downstream (~ 10^3 -10^4 km) from the shock front, where they have cooled below the Curie point of kamacite. If the rate of magnetic diffusion is high, the magnetic field behind the shock will diffuse laterally and will have returned to the background magnetic field of the nebula, B_{bkgrnd}. If the rate of magnetic diffusion is low, the magnetic field strength will simply scale with the gas density, and could be as high as 10-30 B_{bkgrnd} [1,4]. The magnetic field recorded by the chondrules will lie between these two values, depending on how much the magnetic field has diffused laterally.

The goal of this abstract is to explore how much the magnetic field diffuses behind the bow shock around a planetary embryo, and to relate the magnetic field strength recorded by chondrules to the background magnetic field strength of the solar nebula.

Bow shock model: We model the density and temperature of gas behind a planetary bow shock using the code and assumptions of [7]. In the calculations presented here we assume a planet with radius R = 3000 km moving at 7 km/s through nebular gas with density $\rho = 1 \times 10^{-9}$ g cm^{-3} and temperature T = 300 K. An adiabatic equation of state is assumed. The simulation is evolved for ~ 10^6 s until a steady state is achieved. Representative temperatures are shown in Figure 1.

Ionization state: The magnetic diffusion rate depends on the gas ionization and its temperature. Behind a planetary bow shock T >800 K, the temperature at which thermal ionizations---due to gas-phase collisional ionization of potassium atoms, and thermionic emission of electrons and ions from solids---become important [8]. We calculate the ionization state using the code and formulism of [8], constructing a lookup table for the densities of electrons and K^+ ions as a function of density and temperature. In the relevant regime, adsorption and emission of charges from the surfaces of dust grains and chondrules will dominate over gas-phase reactions, and the ionization state is insensitive to the surface area of particles. We assume a solids/gas mass ratio of 0.01, a grain radius 1 μm, and a particle work function of 5 eV. At temperatures above ≈1500-

2000 K, the ionization state is adequately described by the Saha equation.

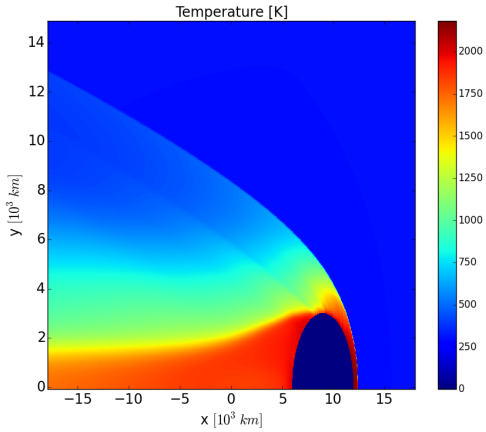

Figure 1: Gas temperature in a planetary bow shock.

Magnetic diffusion rate: We calculate the magnetic diffusion rate using standard formulas [e.g., 9] to relate electron and ion densities to electrical conductivities, combining these with gyrofrequencies and collision timescales of individual species to calculate the rates of magnetic diffusion parallel (D_{parl}) and perpendicular (D_{perp}) to the field. We use the momentum transfer rates of [10]. The diffusion coefficient D_{parl} is associated only with Ohmic dissipation, while D_{perp} is associated with the combined actions of Ohmic dissipation and ambipolar diffusion. In general, D_{perp} - D_{parl} scales as B^2, meaning that strong fields can enhance magnetic diffusion. We assume B=0.5 G.

Results: Figure 2 shows the calculated values of D_{perp} and D_{parl} in the gas behind the shock in Figure 1. In general, because of thermal ionizations, D_{parl} decreases with rising temperature, being as low as 10^{10} cm^2 s^{-1} in the hottest gas in front of the planet, remaining < 3 x 10^{13} cm^2 s^{-1} within a cylinder with radius ~3000 km behind the planet, attaining much higher values farther from the planet. For this diffusion coefficient, the timescale for the field to diffuse laterally significantly is $t_{diff} \sim R^2 / D_{parl} \sim (3000\ km)^2 / (3 \times 10^{13}\ cm^2\ s^{-1}) \sim 3 \times 10^3$ s. For comparison, the timescale for the post-shock gas to flow past the planet is ~ R/V ~ (3000 km) / (1 km/s) ~ 3 x 10^3 s. We conclude that under the action of Ohmic dissipation alone, the magnetic field is frozen into the gas and can remain amplified and compressed, in the cylinder with radius ~ 3000 km behind the planet. Outside of this cylinder, the magnetic field quickly drops to the background field strength ~ 0.5 G. Diffusion of the field perpendicular to B, described by D_{perp}, is an order of magnitude higher than D_{parl} at B=0.5 G, and would be even higher at larger B.

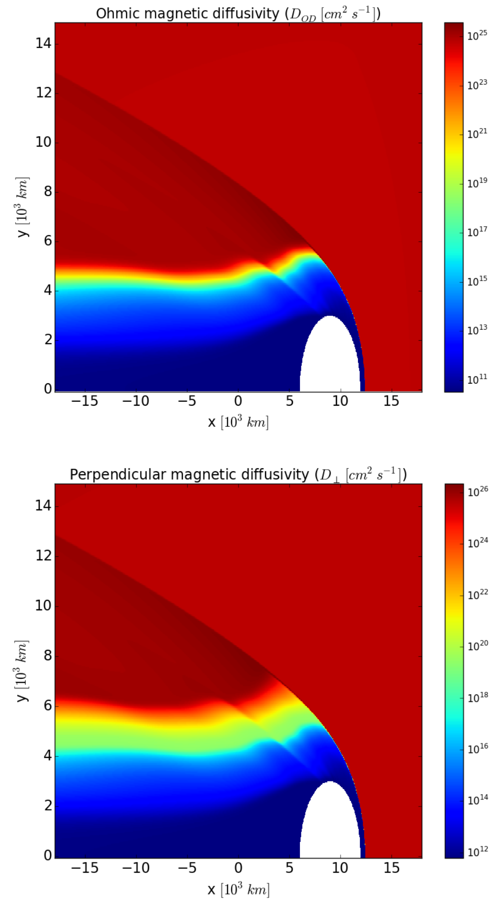

Figure 2: Magnetic diffusion terms D_{parl} (top) and D_{perp} (bottom) in gas behind the planetary bow shock.

Conclusions: In future work we will consider the complications of radiative (non-adiabatic) cooling, evaporation of dust, and ionization kinetics. We will use similar calculations of D_{parl} and D_{perp} to evolve the magnetic field behind the shock, to calculate the magnetic field strength recorded by chondrules as they cool through their Curie points.

Acknowledgements: We gratefully acknowledge support from NASA Emerging Worlds (PI Ben Weiss). ACB acknowledges NSERC, CRC, and CFI.

References: [1] Fu, R.R. et al. 2014, *Science* 346, 1089. [2] Fu, R.R., Weiss, B.P. & Schrader, D.L. 2015, LPSC 46, 1587. [3] Desch, S.J., et al. 2012, *MAPS* 47, 1139. [4] Desch, S.J. & Connolly, Jr., H.C. 2002, *MAPS* 37, 183. [5] Morris, MA. & Desch, S.J. 2010, *ApJ* 722, 1474. [6] Morris, M.A., et al. 2012, *ApJ* 752, 27. [7] Boley, A.C., Morris, M.A. & Desch, S.J. 2013, *ApJ* 776, 101. [8] Desch, S.J. & Turner, N.J. 2015, *ApJ* 811, 156. [9] Desch, S.J. & Mouschovias, T.Ch. 2001, *ApJ* 550, 314. [10] Pinto, C. & Galli, D. 2008, *A&A* 484, 17.